Application of Fractional Calculus to the Sound Waves Propagation in Rigid Porous Materials: Validation Via Ultrasonic Measurements

Zine El Abiddine Fellah, Claude L. Depollier, Mohamed Fellah

Application of fractional calculus to the sound waves propagation in rigid porous materials : validation via ultrasonic measurements

Z.E.A Fellah†, C. Depollier†, M. Fellah‡

† *Laboratoire d'Acoustique de l'Université du Maine, IAM UMR-CNRS 6613, A^ve O. Messiaen 72085 Le Mans Cedex 9, France*
E − mail : zine@laum.univ − lemans.fr.

‡ *Laboratoire de Physique Théorique, Institut de Physique, USTHB BP 32 El Alia Bab Ezzouar 16111, Algérie*

Abstract: This paper starts by summarizing the basic equations of a theoretical model, recentely published by Fellah and Depollier [1], which describes the propagation of pulses in the time domain through a porous medium. In the field of absorbing acoustical porous media, the predictive equations have always been written in the frequency domain. The new method that is proposed is based on the concept of fractional derivatives. The added value of the present work consists in a fine experimental validation performed in plastic foams, sandy sediments and on multilayered porous materials.

1 Introduction

The propagation of sound in fluid saturated porous media with a rigid solid frame is of great interest for a large class of industrial applications. With air as the saturating fluid, potential application of porous air filled solids can be found in noise control, architectural acoustics or in transportation. Some of the recent progresses in this area are reviewed in Allard [2] and Lafarge [3]. Many applications like medical imaging or inverse scattering problems require the study of the behaviour of pulses traveling into porous media [4], it is only recently that the response of these media to such excitations has been fully adressed in Fellah and Depollier [1] for some elementary configuration in porous media. To efficiently cope with the specific problems appearing in the transient acoustic field propagation, new methods are required. At

present, most analysis of signal propagation are carried out in the frequency domain using the Fourier transform to translate the results in the time domain and vice-versa. This, however has several limitations. The first is that the transformation is difficult to compute numerically with sufficient accuracy for non analytical functions. For example, using Fourier transform to obtain time domain results for a lossy material is a more complicated approach than using a true time domain analysis, and the numerical results are less accurate. The second disavantage is that by working in the frequency domain Some physical informations are lost or hard to recover. For exemple, in case of noisy data it may be difficul to reconstruct the chronological events of a signal by phase unwrapping. Consequently, it is difficult to obtain a deep understanding to transient signal propagation using frequency domain method.
The time domain response of the material is described by an instantaneous response and a "susceptibility" kernel responsible for the memory effects. A time domain approach differs from the frequency analysis in that the suceptibility functions of the problem are convolution operators acting on the velocity and the pressure fields, and therefore a different algebraic formalism has to be applied to solve the wave equation. In the past many authors have used the fractional calculus as an empirical method to describe the properties of viscoelastic materials, e.g. in Caputo [5], Bagley [6]. The observation that the asymptotic expressions of stiffness and damping in porous materials are proportional to fractional powers of frequency suggests the fact that time derivatives of fractional order might describe the behaviour of sound waves in this kind of materials, including relaxation and frequency dependence.
The outline of this paper is as follows. In section 2, the model of equivalent fluid is presented and the usual basic equations written in the frequency domain are given. Section 3 is devoted to the connection between the fractional derivatives and wave propagation in rigid porous media. Section 4 contains the high frequency approximation and the time domain equations. Section 5 is devoted to ultrasonic measurements, compared to simulation on plastic foams, sand sample and multilayers.

2 Model of the equivalent fluid

Let a homogeneous isotropic porous material with porosity ϕ be saturated with a compressible and viscous fluid of density ρ_f and viscosity η. It is assumed that the frame of this porous solid is not deformable when it is subjected to an acoustic wave. It is the case for example for a porous medium which has a large skeleton density or very large elastic modulus or weak fluid-structure coupling. To apply the results of continuum mechanic it is required that the wave-length of sound waves should be much larger than the sizes of pores or grains in the medium.
In such porous materials, acoustic waves propagate only in the fluid so, it can be seen as an equivalent fluid, the density and the bulk modulus of which are "renormalized" by the fluid-structure interactions. A prediction of the acoustic comportement of the porous material requires the determination of the dynamic tortuosity $\alpha(\omega)$ and dynamic compressibility $\beta(\omega)$. Theses functions depends to the physical characteristic of the fluid in the pore space of the medium and are independant of the dynamic characteristic of the structure. The basic equations of the model of equivalent fluid are the Euler equation (E) and a constitutive equation (M) obtained from the equation of mass conservation associated with the behaviour (or adiabatic) equation and we will henceforth refer to them as EM equations

$$\rho_f \alpha(\omega) \frac{\partial v_i}{\partial t} = -\nabla_i p, \quad \frac{\beta(\omega)}{K_a} \frac{\partial p}{\partial t} = -\nabla . \mathbf{v}. \tag{1}$$

In these relations, $\mathbf{v}$ and p are the particle velocity and the acoustic pressure, $K_a = \gamma P_0$ is the compressibility modulus of the fluid, $\alpha(\omega)$ and $\beta(\omega)$ are the dynamic tortuosity of the medium and the dynamic compressibility of the air included in the porous material. These two response factors are complex functions which heavily depend on the frequency $f = \omega/2\pi$. Their theoretical expressions are given by Allard [2] and Lafarge [3] :

$$\alpha(\omega) = \alpha_\infty \left(1 + \frac{\eta\phi}{j\omega\alpha_\infty\rho_f k_0}\sqrt{1 + j\frac{4\alpha_\infty^2 k_0^2 \rho_f \omega}{\eta\Lambda^2\phi^2}}\right), \tag{2}$$

$$\beta(\omega) = \gamma - (\gamma - 1)\left(1 + \frac{\eta\phi}{j\omega\rho_f k_0' Pr}\sqrt{1 + j\frac{4k_0'^2\rho_f\omega Pr}{\eta\phi^2\Lambda'^2}}\right)^{-1}, \tag{3}$$

where $j^2 = -1$, γ represents the adiabatic constant, Pr the Prandtl number, α_∞ the tortuosity, k_0 the static permeability, k_0' the thermal permeability, Λ and Λ' the viscous and thermal characteristic lengths [8]. This model was initially developped by Johnson [9], and completed by Allard [10] by adding the description of thermal effects Later on, Lafarge [3] has introduced the parameter k_0' which describes the additional damping of sound waves due to the thermal exchanges between fluid and structure at the surface of the pores.
The functions $\alpha(\omega)$ and $\beta(\omega)$ express the viscous and thermal exchanges between the air and the structure which are responsible of the sound damping in acoustic materials. These exchanges are due on the one hand to the fluid-structure relative motion and on the other hand to the air compressions-dilatations produced by the wave motion . The parts of the fluid affected by these exchanges can be estimated by the ratio of a microscopic characteristic length of the media, as for example the sizes of the pores, to the viscous and thermal skin depth thickness $\delta = (2\eta/\omega\rho_0)^{1/2}$ and $\delta' = (2\eta/\omega\rho_0 P_r)^{1/2}$. For the viscous effects this domain corresponds to the region of the fluid in which the velocity distribution is perturbed by the frictional forces at the interface between the viscous fluid and the motionless structure. For the thermal effects, it corresponds to the fluid volume affected by the heat exchange between the two phases of the porous medium.
The sound velocity in the porous material is derived from equations (2) and (3) and yields the usual equation :

$$c(\omega) = \sqrt{\frac{K_a}{\rho_f \alpha(\omega)\beta(\omega)}}. \tag{4}$$

In this expression, the velocity is a complex function of the frequency which is not very convenient in order to investigate the propagation of ultrasonic short pulses or to deduce the values of the parameters of the medium. This is due to the fact that the EM equations are neither expressed in time-domain nor in frequency-domain: they are correct only for monochromatic waves. To restore their validity for transient signals, we need to write them in the time-domain.

3 Wave equations in the time-domain

When a sound wave propagates in a porous medium saturated by a fluid its behaviour radically changes according to the frequency [1]. At low frequency, the wave motion is determined by viscous effects, while inertial effects are dominating at high frequency. Only the high frequency response is considered in the following approximation.

3.1 High frequency approximation

When the wave frequency is high, the skin depth is very narrow and the viscous effects are concentrated in a small volume near the frame $\delta/r \ll 1$; then the viscous effects in the fluid can be neglected: the fluid behaves almost like a perfect fluid (without viscosity).
In the same way, the compression/dilatation cycle is a much faster process than the heat transfer between the air and the structure and it is a well-founded approximation to consider that the compression is adiabatic. In The high frequency approximations of the response factors $\alpha(\omega)$ et $\beta(\omega)$ when $\omega \to \infty$ are then given by the relations:

$$\alpha(\omega) \approx \alpha_\infty \left(1 + \frac{2}{\Lambda}\left(\frac{\eta}{j\omega\rho_f}\right)^{1/2}\right), \tag{5}$$

$$\beta(\omega) \approx 1 + \frac{2(\gamma-1)}{\Lambda'}\left(\frac{\eta}{j\omega Pr\rho_f}\right)^{1/2}. \tag{6}$$

In the time-domain the expressions of the responses α and β are given by Fellah and Depollier [1] :

$$\alpha(\omega) \xrightarrow{t} \tilde{\alpha}(t) = \alpha_\infty\left(\delta(t) + \frac{2}{\Lambda}\left(\frac{\eta}{\rho_f}\right)^{1/2} t^{-1/2}\right)\star, \tag{7}$$

$$\beta(\omega) \xrightarrow{t} \tilde{\beta}(t) = \left(\delta(t) + \frac{2(\gamma-1)}{\Lambda'}\left(\frac{\eta}{Pr\rho_f}\right)^{1/2} t^{-1/2}\right)\star, \tag{8}$$

where $\star$ denotes the time convolution and $\delta(t)$ is the Dirac function. In this model $t^{-1/2}$ is interpreted as a semi-derivatives operator following the definition of the fractional derivatives of order ν given by Samko *et al* [11],

$$D^\nu[x(t)] = \frac{1}{\Gamma(-\nu)}\int_0^t (t-u)^{-\nu-1}x(u)du, \tag{9}$$

where $\Gamma(x)$ is the gamma function.
In this framework, the basic equations EM of the model can be written as

$$\rho_f\tilde{\alpha}(t)\star\frac{\partial v_i}{\partial t} = -\nabla_i p \qquad and \qquad \frac{\tilde{\beta}(t)}{K_a}\star\frac{\partial p}{\partial t} = -\nabla.v, \tag{10}$$

When the wave propagates along the coordinate axis ox, Eq. 1 are generalized as follows in the time-domain:

$$\rho_f\alpha_\infty\frac{\partial v}{\partial t} + 2\frac{\rho_f\alpha_\infty}{\Lambda}\left(\frac{\eta}{\pi\rho_f}\right)^{1/2}\int_{-\infty}^t \frac{\partial v/\partial t'}{\sqrt{t-t'}}dt' = -\frac{\partial p}{\partial x}, \tag{11}$$

$$\frac{1}{K_a}\frac{\partial p}{\partial t} + 2\frac{\gamma-1}{K_a\Lambda'}\left(\frac{\eta}{\pi Pr\rho_f}\right)^{1/2}\int_{-\infty}^t \frac{\partial p/\partial t'}{\sqrt{t-t'}}dt' = -\frac{\partial v}{\partial x}. \tag{12}$$

A consequence of this result is that the retarding force is no longer proportional to the time derivative, it is found to be proportional to a fractional derivative of order 1/2 of the acoustic

velocity. This occurs because the volume of fluid participating to the motion is not the same for all motion, as it is for a fully developed steady flow. The phenomena may be understood by considering such a volume of fluid in a pore to be in harmonic motion. At a high frequency, only a thin boundary layer is excited: the average shear stress is high. At a lower frequency, the same amplitude of the fluid motion allows a thicker layer of fluid to participate in the motion and consequently the shear stress is less. The penetration distances of the viscous forces and therefore the excitation of the fluid depends on frequency. In the time domain, such a dependance is associated with a fractional derivative. The generalized mass conservation equation is interpreted in the same way. In these equations, the convolutions express the dispersive nature of the porous material. They take into account the memory effects due to the fact that the response of the medium to the wave excitation is not instantaneous but needs some time to take place.
The wave equation is derived from these two relations by elementary calculations and can be written as :

$$\frac{\partial^2 v}{\partial x^2} - A\frac{\partial^2 v}{\partial t^2} - B\int_{-\infty}^{t} \frac{\partial^2 v/\partial t'^2}{\sqrt{t-t'}}dt' - C\frac{\partial v}{\partial t} = 0, \tag{13}$$

where the coefficients are given by:

$$A = \frac{\rho_f \alpha_\infty}{K_a}, \quad B = \frac{2\alpha_\infty}{K_a}\sqrt{\frac{\rho_f \eta}{\pi}}\left(\frac{1}{\Lambda} + \frac{\gamma-1}{\sqrt{Pr}\Lambda'}\right) \quad C = \frac{4\alpha_\infty(\gamma-1)\eta}{K_a \Lambda\Lambda'\sqrt{Pr}}.$$

The first one gives the velocity $c = A^{-1/2}$ of the wave in the air included in the porous material. In this case the fluid density is modified by the factor α_∞. The other coefficients are essentially dependent of the characteristic lengths Λ and Λ' and express the viscous and thermal interactions between the fluid and the structure. The knowledge of these three coefficients allows the determination of the three parameters α_∞, Λ and Λ'. This can be achieved from the measurements of the damping and broadening of ultrasonic pulses during the propagation in the porous medium.
Inverse problems yielding the determination of α_∞, Λ and Λ' are not treated here. The direct problem is validated by measurements on materials in the high frequency domain. Parameters of theses materials are known by previous validated methods. Numerical simulations using the present model and these parameters are compared to the measurements.

4 Ultrasonic measurements

Experiments are done in air with two broadband Panametrics V389 piezoelectric transducers having a 250 kHz central frequency in air and a bandwith at 6 dB extending from 60 to 420 kHz. Pulses of 900V are provided by a 5058PR Panametrics pulser/receiver (see Fig. 1).
Received signals are amplified up to 90 dB and filtered above 1 MHz to avoid high frequency noise (energy is totally filtered by the sample in this upper frequency domain).
Electronics perturbations are removed by 1000 acquisition averages.

Measurements have been performed on plastic foams and sand samples with various flow resistivities. Plastic foams were provided by Recticel (Belgium). The parameters for these materials are given in Table 1. First row of Table 1 gives the values of the parameters for the foam $F1$ determined by the method [14] (values marked by $*$). The other values are given by optimization with our model. The last column of Table 1 gives frequency $f_{0.1}$ for which $\delta/\Lambda = 0.1$. This frequency is an indicator of the high frequency approximation. It shows that for the foams F1

and F3 for which the flow resistivity is low, the high frequency approximation is effective as soon as the frequency is an order of several kilohertz, on the other hand, for the foam F2, this approximation is reached for a much higher frequency (150 Khz). At frequencies below 30 kHz, no filtering occurs.
In the case of sand as compared to foams, because of a low upper cut-off frequency, it is necessary to send more energy in a lower frequency domain. A pulse (burst of one period) centered at 120 kHz is therefore provided by a 33120A Hewlett Packard function generator and passed by a 50dB-[10kHz-10MHz] high power amplifier. This improves the emission efficiency of the transducers in the range [60-150] kHz. At 120 kHz , the ratio $\delta/\Lambda = 0.28$ shows that only a part of the signal frequency range satisfies the high frequency approximation.

4.1 Comparison between measurements and simulations

Simulated signals are obtained from the convolution of the Green function of the propagation equation (16) given in Ref. [13] with the experimental reference signal. The reference signal for the foams F1 and F2 is given in figure fig.2. A comparison between predicted signal calculated from the values of the parameters given by method [14] for F1 and experimental signal is presented on fig.3. Fig.4 compairs the same experimental results with predicted signal calculated with parameters obtained by optimization from our model. The general shape of the predicted signal is exactely respected in both figure 3 and 4. However in fig.3, the amplitude and the position of the maximum of the predicted signal does not fit the experimental data as it does on fig.4. Fig.5 presents the same results than fig.4 for the optimized parameters for F2. In spite of fact that the flow resistivity is high, our model gives results which are in good agreement with experimental data.
The similar study was made for sand samples (sand characterization has a great importance in submarine research). Its high tortuosity and resistivity, due to small grains obstructing the pores, and its weak porosity makes this material much different from foams. Moreover, grains with large size creates scattering phenomenon and increases damping. In order to reduce scattering, sand is filtered and only grains of size lower than 500 μm are kept. Reference signal is a 120 kHz (instead of 250 kHz) centered pulse because of a low upper cut-off frequency for sand. The reference signal is given in fig.6, the comparison between predicted signal (with optimized parameters) and experimental signal is given in figure 7; parameters are optimized with our model. The agreement is correct, but less precise than for the foams. This may be due to the incertitude on the thikness of the sample (its irregular surface at small thikness) and to the fact that lowest part of the signal spectrum is out of the range of the high frequency approximation. Multilayered structure have also been studied. The foams F1 and F3 (Table 1) are simply "put" one over each other. They are not glued and not constrained. Simulated signal is obtained by taking as input, for each layer, the output of the previous layer. Agreement is fairly good. Fig.8 gives a comparison between predicted and experimental results.

5 CONCLUSION

In this paper an experimental validation for a theoretical model based on fractional derivatives concept for pulses propagation in the time domain through porous media is given. A good agreement between theory and experience is observed for different materials (such as foams and sand) in a large range of air flow resistivity. An application to multilayered media let us a hope

to treat inhomogeneous media. The direct problem for the propagation is well solved and we hope now to work out the inverse problem in order to determinate the high frequency parameters α_∞, Λ and Λ' from the propagation.

References

[1] Z.E.A. Fellah and C.Depollier: Transient acoustic wave propagation in porous media: a time-domain approach, J. Acoust. Soc, **107**, 683-688, (2000)

[2] J.F. Allard: Propagation of Sound in Porous Media : Modeling Sound Absorbing Materials, Chapman and Hall, London, (1993).

[3] D. Lafarge: Propagation du son dans les matériaux poreux à structure rigides saturés par un gaz. Ph.D. Dissertation, Université du Maine, (1993).

[4] L. Päivärinta, and E Somersalo (Eds): Inverse Problems in Mathematical Physics, Springer, Berlin, (1993). Mir Publishers, Moscow, (1980).

[5] M. Caputo: Vibrations of an infinite plate with a frequency independent Q, J. Acoust. Soc. Am. **60**, 632-637, (1976).

[6] R.L. Bagley and P.J. Torvik: On the fractional calculus Model of Viscoelastic Behavior, Journal of Rheology, **30**, 133-155, (1983).

[7] C. Zwikker and C.W. Kosten: Sound absorbing materials, Elsevier, New York, (1949).

[8] D. Lafarge, J.F. Allard, B. Brouard: Characteristic dimensions at high frequencies of the surface impedance of porous layers, J. Acoust, Soc. Am. **93**, 2474-2478, (1993).

[9] D.L. Johnson, J. Koplik, R. Dashen: Theory of dynamic permeability and tortuosity in fluid-saturated porous media, J. Fluid.Mech. **176**, 379-402, (1987).

[10] J.F. Allard, Y. Champoux: New empirical equations for sound propagation in rigid frame fibrous materials, J. Acoust. Soc. Am. **91** 3346-3353, (1992).

[11] S. G. Samko, A.A. Kilbas and O.I. Marichev, Fractional Integrals and Derivatives : Theory and Applications, Gordon and Breach Science Publishers,Amsterdam, (1993).

[12] P. Leclaire, L. Kelders, W. Lauriks, N.R. Brown, M. Melon , B. Castagnède: Determination of the viscous and thermal characteristics lengths of plastics foams by ultrasonic measurements in helium and air, J. Appl. Phys. **80**, 2009-2012, (1996).

[13] Z.E.A. Fellah, C.Depollier and M. Fellah: An approach to direct and inverse time-domain scattering of acoustic waves from rigid porous materials by a fractional calculus based method, Journal of Sound and Vibration, to appear.

[14] N. Brown, M. Melon, V. Montembault, B. Castagnède, W. Lauriks and P. Leclaire: Evaluation of viscous characteristic length of air-saturated porous materials form the ultrasonic dispersion curve, C. R. Acad. Sci. Paris, bf 322, série II p. 121, (1996).

FIGURE CAPTIONS

Fig. 1. Experimental set-up of the ultrasonic measurements. Two signals are obtained with and without sample. the system is used vertically to study multilayers.

Fig. 2. Incident signal for the Foams F1 and F2.

Fig. 3. Experimental signal (dashed line) and predicted signal (continuous line) for the foam F1 (parameters given by Brown *et al* method).

Fig. 4. Experimental signal (dashed line) and predicted signal (continuous line) for the foam F1 (parameters optimized parameters).

Fig. 5 . Experimental signal (dashed line) and predicted signal (continuous line) for the foam F2 (parameters optimized parameters).

Fig. 6. Reference signal for the sand.

Fig. 7. Experimental signal (dashed line) and predicted signal (continuous line) for sand (optimized parameters).

Fig. 8. Experimental signal (dashed line) and predicted signal (continuous line) for a multilayer constituted by F1 (1cm), F2 (1cm), F1 (1cm), F2 (2cm) (optimized parameters).

Table 1 : Porous media used for measurement and reference parameters used simulations.

Material	Thickness (cm)	ϕ	σ (10^3 Nm^{-4}s)	α_∞	Λ (μm)	Λ' (μm)	$f_{0.1}$ (kHz)
Foam F1	5	0.98	9	1.04*	200*	600*	11.93
Foam F1	5	0.98	9	1.053	208	620	11.03
Foam F2	1.1	0.92	38	1.24	45	135	157.83
Foam F3	5	0.97	2.85	1.05	300	750	5.3
Sand	0.7	0.4	170	1.65	22	60	

S

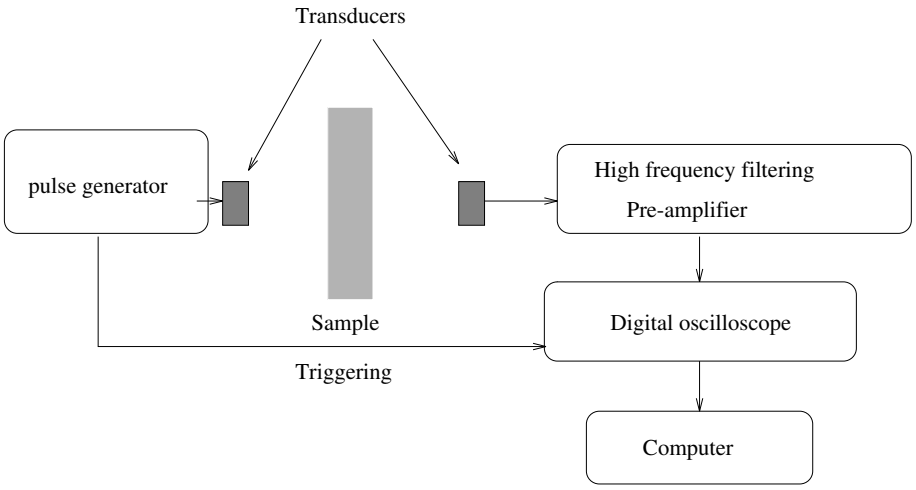
Transducers
pulse generator
High frequency filtering
Pre-amplifier
Sample
Digital oscilloscope
Triggering
Computer

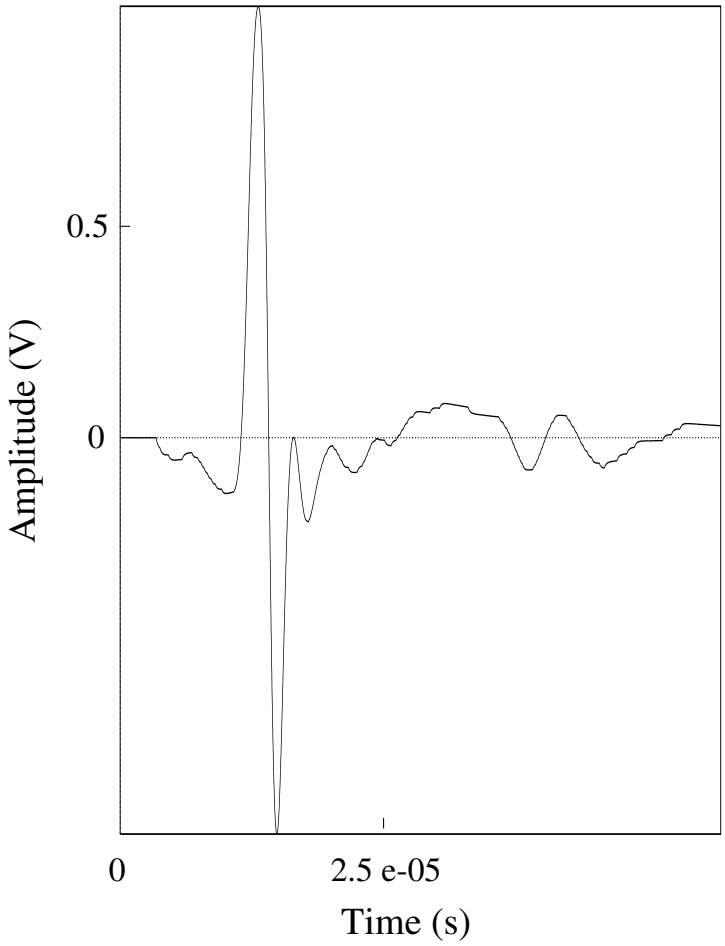
0.5
0
Amplitude (V)
0
2.5 e-05
Time (s)

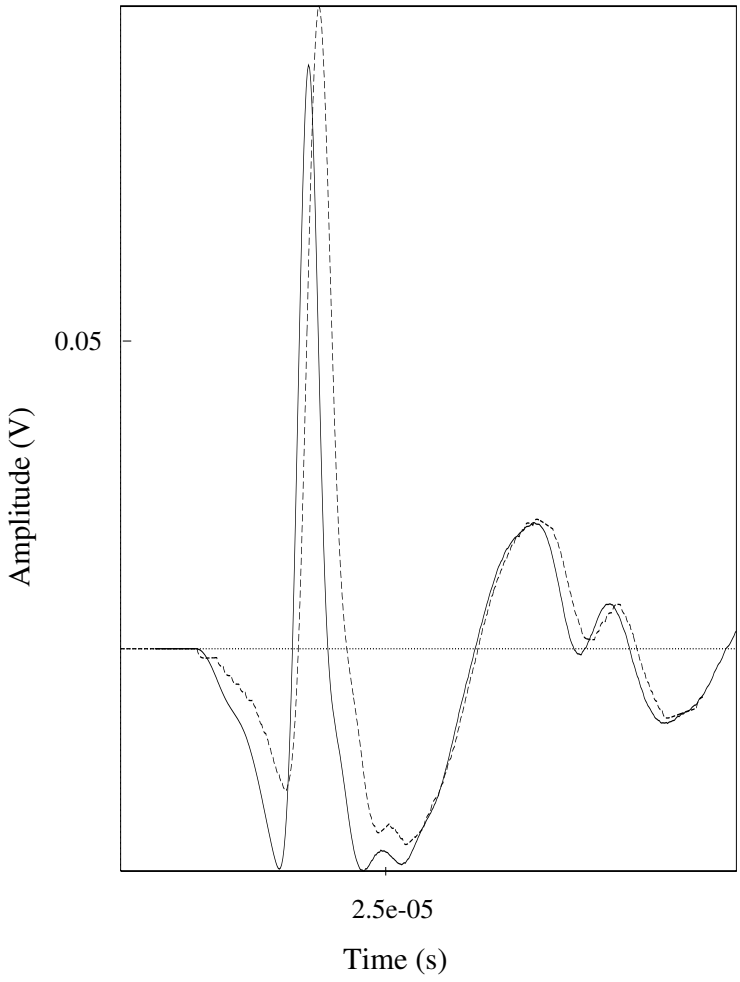
0.05
Amplitude (V)
2.5e-05
Time (s)

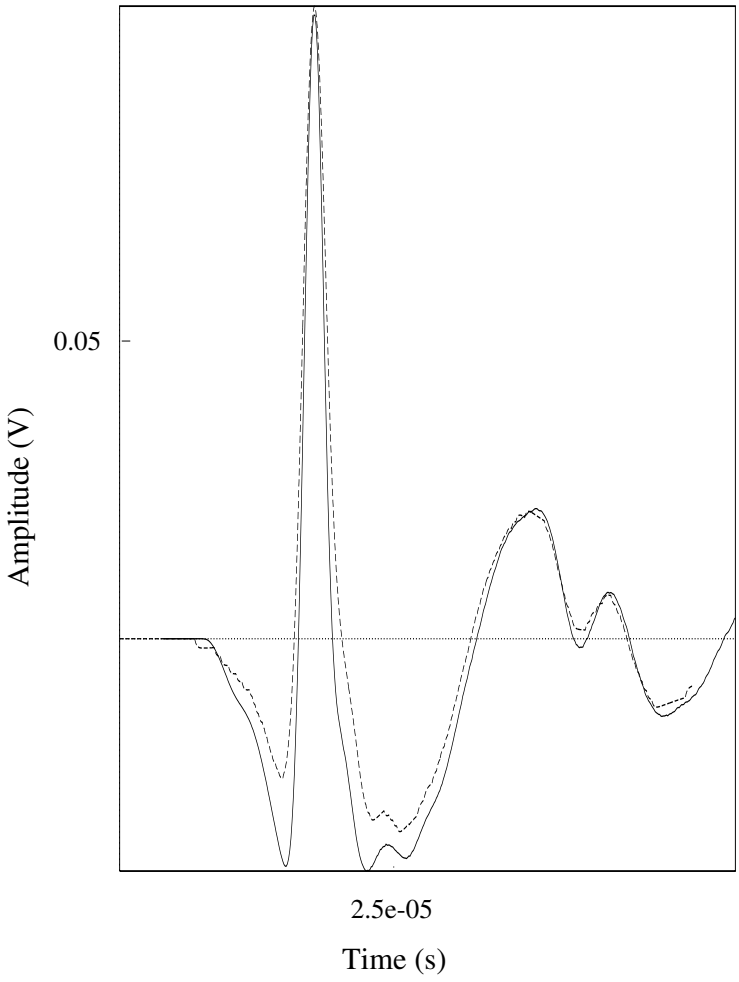
0.05
Amplitude (V)
2.5e-05
Time (s)

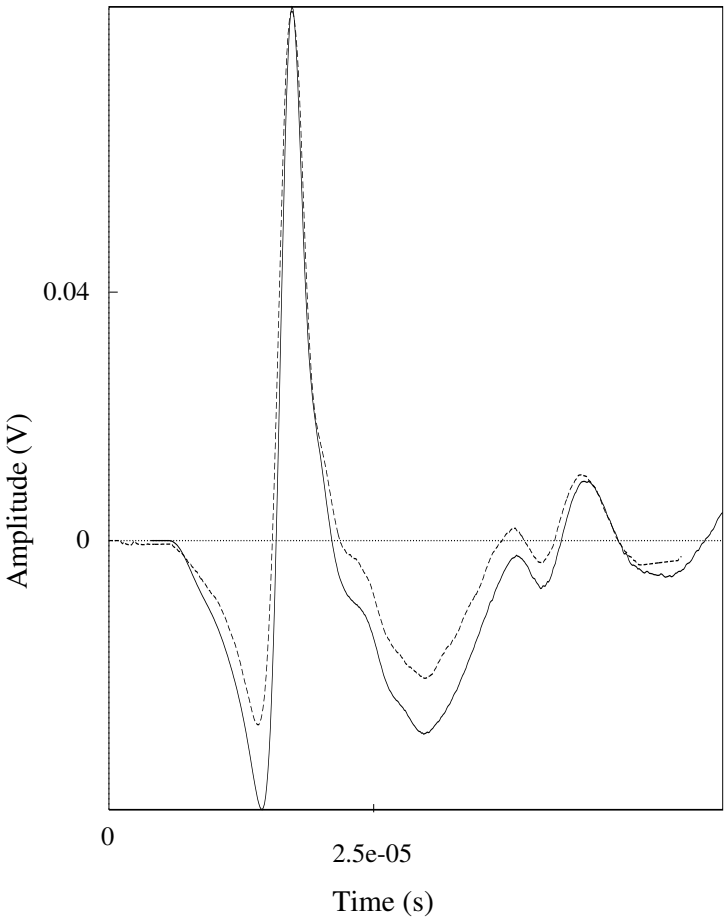
0.04
0
Amplitude (V)
0
2.5e-05
Time (s)

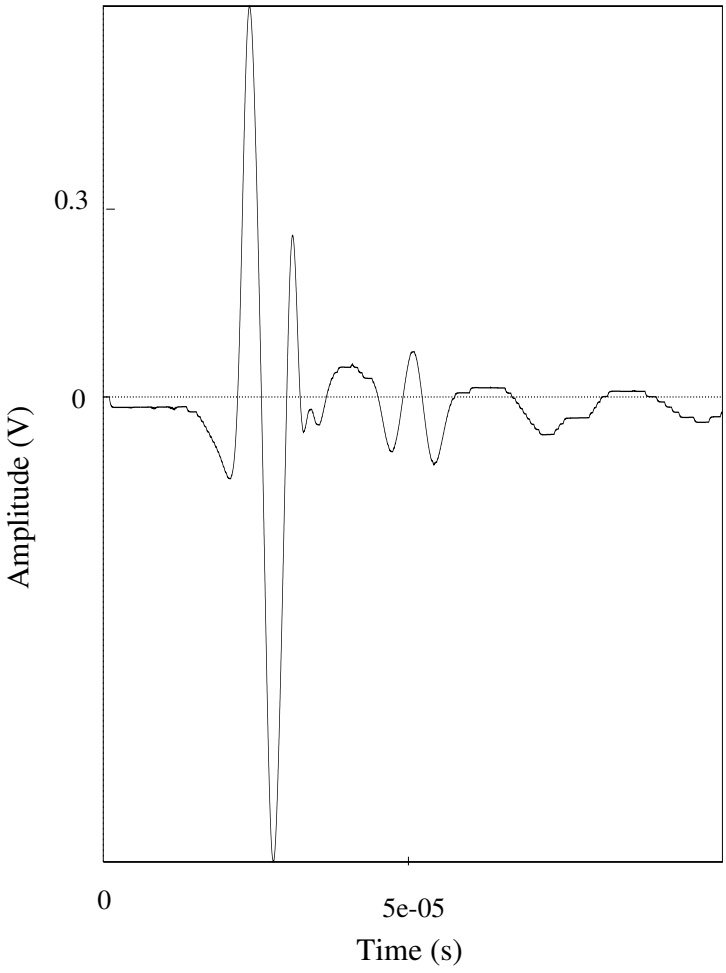
0.3
0
Amplitude (V)
0
5e-05
Time (s)

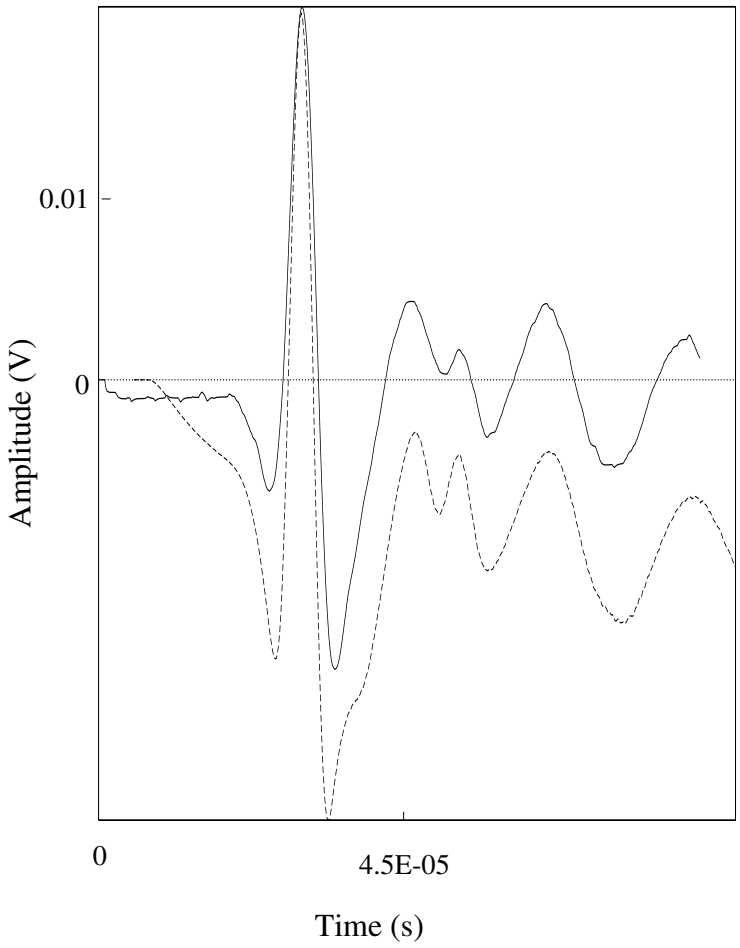
0.01
0
Amplitude (V)
0
4.5E-05
Time (s)

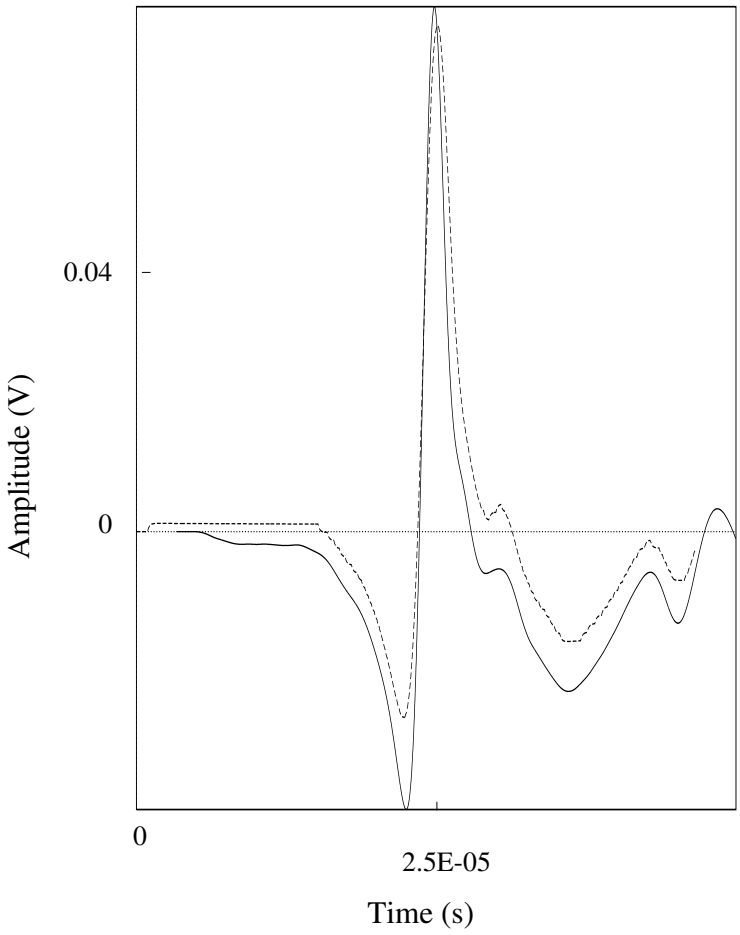
0.04
0
Amplitude (V)
0
2.5E-05
Time (s)